NANO LETTERS

Letter

pubs.acs.org/NanoLett

Formation of Nanometer-Sized Surface Platinum Oxide Clusters on a Stepped Pt(557) Single Crystal Surface Induced by Oxygen: A High-Pressure STM and Ambient-Pressure XPS Study

Zhongwei Zhu,[†,‡] Franklin (Feng) Tao,[§] Fan Zheng,[‡] Rui Chang,[∥] Yimin Li,[†,‡] Lars Heinke,[‡] Zhi Liu,[∥] Miquel Salmeron,[‡,⊥] and Gabor A. Somorjai*[,†,‡]

[†]Department of Chemistry, University of California, Berkeley, California 94720, United States

[‡]Materials Sciences Division, Lawrence Berkeley National Laboratory, Berkeley, California 94720, United States

[§]Department of Chemistry and Biochemistry, University of Notre Dame, Notre Dame, Indiana 46556, United States

[∥]Advanced Light Source, Lawrence Berkeley National Laboratory, Berkeley, California 94720, United States

[⊥]Department of Materials Science and Engineering, University of California, Berkeley, California 94720, United States

S *Supporting Information*

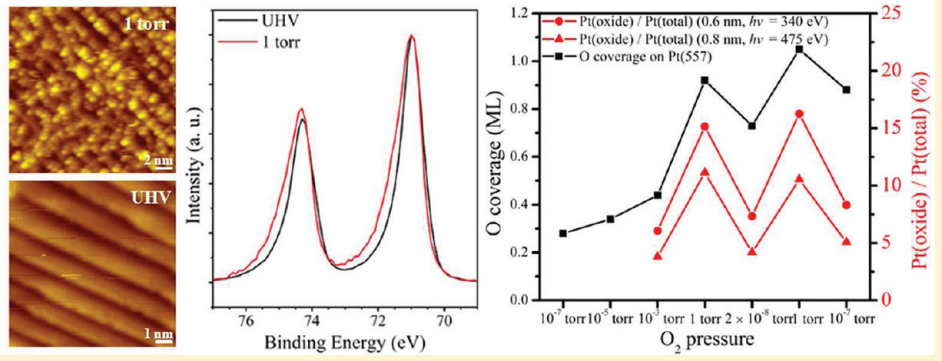

ABSTRACT: We studied the oxygen-induced restructuring process on a stepped Pt(557) single crystal surface using high-pressure scanning tunneling microscopy (HP-STM) and ambient-pressure X-ray photoelectron spectroscopy (AP-XPS) at O_2 pressures up to 1 Torr. HP-STM has revealed that nanometer-sized clusters are created on Pt(557) at 1 Torr of O_2 and at room temperature. These clusters are identified as surface Pt oxide by AP-XPS. The appearance of clusters is preceded by the formation of 1D chain structures at the step edges. By using a Pt(111) surface as a reference, it was found that the step sites are the nucleation centers for the formation of surface oxide clusters. These surface oxide clusters disappear and the stepped structure is restored on Pt(557) after evacuating O_2 to 10^{-8} Torr. Changes in the surface oxide concentration in response to variations in the O_2 gas pressure are repeatable for several cycles. Our results that small clusters are initiated at step sites at high pressures demonstrate the importance of performing in situ characterization of stepped Pt catalysts under reaction conditions.

KEYWORDS: *Stepped Pt single crystal, HP-STM, AP-XPS, surface oxide*

Heterogeneous catalysts usually contain a large amount of low coordination sites such as steps, kinks, and vacancies, which have long been considered as the active sites during catalytic reactions. These low-coordination sites can influence activity and selectivity of reactions, because they strongly bind with reactants and readily break chemical bonds.[1−7] In addition, a high concentration of unsaturated surface sites can promote substrate reconstruction in response to adsorbed molecules, giving rise to step coalescence,[8−10] microfaceting,[11] and cluster formation.[12]

Recently developed in situ techniques have revealed the relation between catalyst structures and turnover rates under reaction conditions.[13−18] At high gas pressures and elevated temperatures, transition metal surfaces can undergo dramatic structural changes, as a result of the increased coverage of the gas molecules.[12,18−21] High-pressure scanning tunneling microscopy (HP-STM) can provide information regarding local surface electronic structure and morphology at the nanometer scale.[22,23] Ambient-pressure X-ray photoelectron spectroscopy (AP-XPS) allows us to monitor the chemical states of both adsorbed reactants and underlying catalyst surfaces.[24]

Using these techniques, we have recently reported that stepped Pt(557) and Pt(332) crystal surfaces break into nanometer-sized Pt clusters at a CO pressure of 1 Torr.[12]

Received: December 1, 2011
Revised: January 27, 2012
Published: February 2, 2012

These Pt clusters on Pt(557) and Pt(332) were in triangle and parallelogram shapes, respectively. Such surface restructuring was reversible, since clusters disappeared and steps reformed after the CO gas was removed. The dramatic reconstruction to clusters occurred simultaneously with the growth of a high-binding energy component in the Pt 4f XPS spectrum, which was attributed to low-coordinated Pt atoms at cluster edges bonded with CO. Step sites played a central role in inducing the formation of clusters on Pt surfaces, since no clusters were observed on Pt(111) crystal surface under similar CO pressures.[25]

O_2 can oxidize coordinatively unsaturated Pt surfaces at high gas pressures, and therefore also cause profound changes in Pt surface structure. The variety of surface platinum and oxygen chemical states from chemisorption through to surface Pt oxide[26−31] has called for a detailed in situ investigation of the Pt−O system. In this paper, we report the investigation by HP-STM and AP-XPS of the interaction between oxygen and a stepped Pt(557) surface at pressures from 10^{-7} to 1 Torr and at room temperature. We found that in the presence of 1 Torr of O_2, a one-dimensional (1D) chain structure forms first at the step edges, and clusters of approximately 1 nm in size subsequently cover the surface. These clusters are identified as a surface Pt oxide phase by means of AP-XPS. Comparative studies on Pt(111) demonstrate that clusters preferentially form at the step edges at 1 Torr, whereas direct oxidation of terraces is kinetically limited. After evacuation to the 10^{-8} Torr range, most of the clusters disappear in STM images and the surface oxide component seen in XPS spectra is attenuated. The concentration of surface oxide could repeatbly vary with the O_2 pressure for several cycles.

All the STM experiments were carried out in a home-built HP-STM system.[32] The HP-STM system consists of a 19 cm^3 Au-coated STM batch cell that is able to work at pressures of up to 1000 Torr. The STM cell is integrated into an ultrahigh vacuum (UHV) chamber with a base pressure of 8×10^{-11} Torr. A load lock and another UHV chamber for sample preparation (base pressure 1×10^{-10} Torr) are combined in the system.

The Pt(557) and Pt(111) crystals were cleaned through repeated cycles of 1000-eV Ar^+ sputtering at 3×10^{-5} Torr at room temperature for 20 min, oxygen annealing at 5×10^{-8} Torr at 923 K for 3 min and subsequent vacuum annealing at 1073 K for 5 min. The crystals were cooled down to room temperature at a rate of 1 K/sec after the final annealing step. Before experiments, the sample cleanliness was confirmed by absence of C and O in Auger electron spectroscopy (PHI 15-255G double pass cylindrical mirror analyzer).

STM experiments at pressures lower than 10^{-7} Torr were performed by directly dosing the O_2 gas into the STM chamber, which is separated from the rest of system by gate valves. At pressures above 10^{-7} Torr, a bayonet seal was used to isolate the STM cell from the system and simultaneously maintain the STM chamber under vacuum. The pressure inside the cell was measured using a Baratron capacitance gauge (MKS 722A). STM images were recorded using $Pt_{0.8}Ir_{0.2}$ tips with diameters of 0.25 mm (Bruker AFM probes).

AP-XPS experiments were performed on a Scienta 4000 HiPP workstation at Beamline 9.3.2 of the Advanced Light Source (ALS) at Lawrence Berkeley National Laboratory (LBNL).[33,34] The base pressure of this instrument is maintained around 10^{-10} Torr. XPS survey scans were performed to ensure the absence of impurities on the Pt crystal surfaces prior to gas introduction. Pt 4f and O 1s core level spectra were recorded with incident X-ray photon energies of 340 and 800 eV, respectively, in order to generate photoelectrons with similar kinetic energies (~270 eV). Controlling the kinetic energy of the detect electrons ensures the same probing depth for both elements.[35] The Pt 4f region was also studied with 475 eV incident photon energy to detect deeper surface layers. The energy positions of all XPS spectra were calibrated relative to the Fermi edge (set at 0 eV) recorded with the same incident photon energy.

Figure 1 shows a model of a Pt(557) single crystal surface with a 6(111) × (100) structure[36] and the corresponding STM

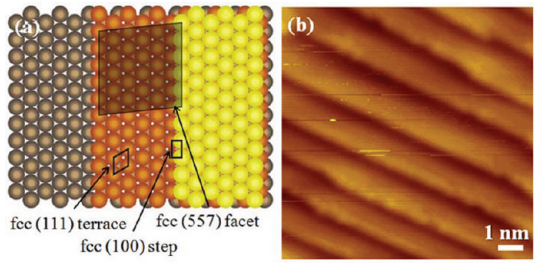

Figure 1. (a) Ball model of a Pt(557) surface. Light yellow, orange, and gray balls represent the top, second, and third layer of Pt atoms, respectively. (b) STM image of Pt(557) taken under UHV conditions (8×10^{-11} Torr). The measured average terrace width is 1.6 nm. Sample bias (V_s) = 0.20 V, tunneling current (I_t) = 0.10 nA, T = 298 K.

image taken in UHV. The measured average terrace width of clean Pt(557) is 1.6 nm from Figure 1b, which is close to the calculated value of 1.4 nm based on the crystal structure.

Figure 2a shows that 30 min after exposure of Pt(557) to 1 Torr of O_2, ordered stripes are resolved on portions of the step edges which remain straight. The line scan in the inset illustrates that the stripes consist of a periodic array of brightness maxima with 250 pm periodicity on average, close to the Pt−Pt distance in the crystal lattice. This structure likely corresponds to a 1D Pt oxide chain, which was reported to form at edges of stepped Pt crystals under high oxygen coverage by means of XPS studies and theoretical calculations.[26,29] Our STM images thus provide direct proof for the existence of 1D oxides on a stepped Pt surface. A few bright elongated structures with an average length of 1.0 nm and an average height of 0.16 nm also form near the Pt oxide chains. Figure 2b, acquired 2 h after introducing 1 Torr of O_2, shows that numerous clusters ~1 nm in diameter and ~0.15 nm in height cover the majority of the surface. These nanometer-sized clusters are roughly aligned along the original steps, suggesting that the clusters are formed by growth from the 1D oxide chain. A further increase of the O_2 pressure to 10 Torr results in a disordered cluster overlayer on the Pt(557) surface. We ascribe the clusters to a 2D surface oxide phase.

The assignment of clusters to surface Pt oxide is supported by AP-XPS experiments in which a Pt(557) crystal was exposed to different O_2 pressures. Figure 3a displays the Pt 4f core level spectra of Pt(557) recorded with 340 eV photon energy in UHV and under 2 h exposure to 1 Torr of O_2. Both the location of the Pt $4f_{7/2}$ peak at 71.0 eV and the spin−orbit splitting of 3.3 eV agree with literature values.[37,38] At 1 Torr of O_2, an additional component appears at 71.6 eV with a core level shift (CLS) of +0.6 eV, as marked in Figure 3a and more

dx.doi.org/10.1021/nl204242s | Nano Lett. 2012, 12, 1491−1497

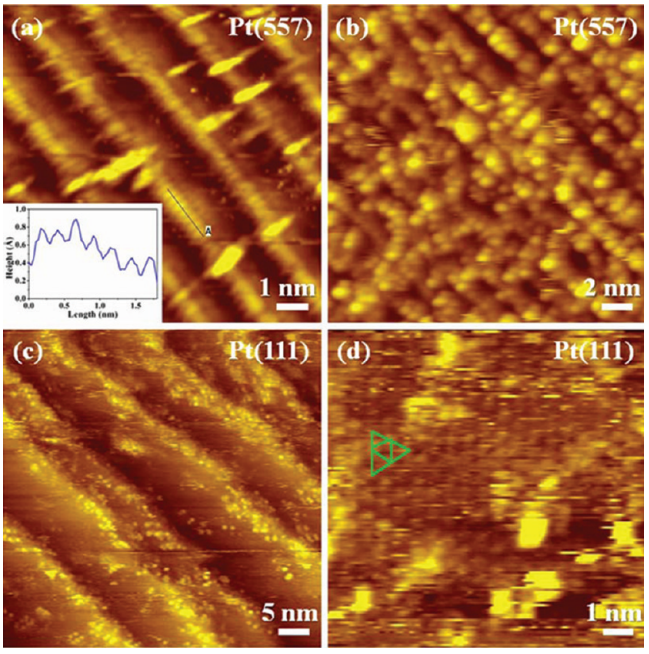

Figure 2. STM images of Pt(557) taken in 1 Torr of O_2 (a) 30 min and (b) 2 h after continuous exposure of the clean Pt(557) to O_2 gas. A periodic 1D chain structure is resolved at the step edges in (a) with the inset showing the line profile, while in (b) disordered clusters of approximately 1 nm in size cover the surface roughly following the original stepped structure. (c,d) Lower and higher magnification STM images of Pt(111) (the few steps indicate a miscut of approximately 1°), acquired after 1.5 h exposure to 1 Torr of O_2. Numerous nanosized clusters accumulate close to the steps on the upper terraces in (c). A chemisorbed oxygen p(2 × 2) pattern, marked by green triangles, is resolved between clusters on Pt(111) terrace, as shown in (d). V_s = 0.20 V, I_t = 0.10 nA, T = 298 K.

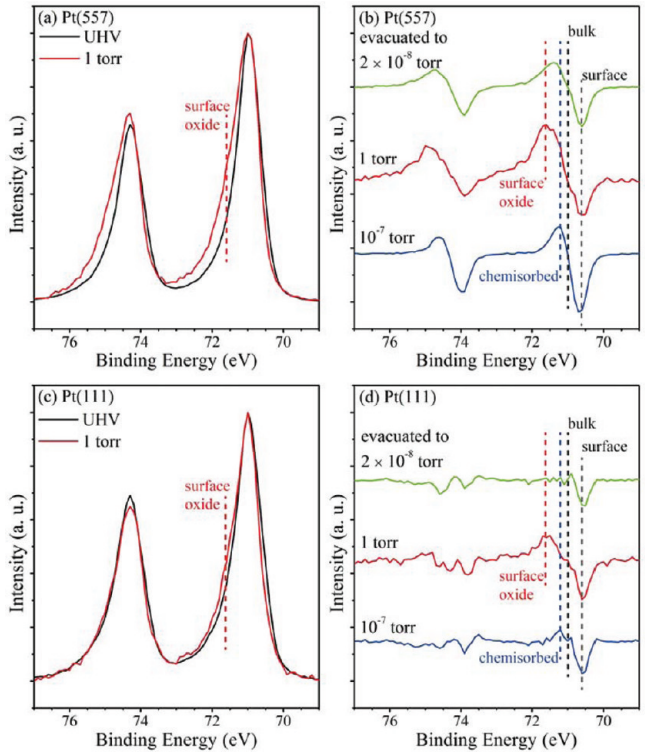

Figure 3. (a) Pt 4f spectra of Pt(557) recorded in UHV and under 2 h exposure to 1 Torr of O_2. A shoulder representing surface Pt oxide arises at +0.6 eV CLS. (b) Difference Pt 4f spectra of Pt(557) acquired under exposure to 10^{-7} Torr of O_2 for 2 h, 1 Torr of O_2 for 2 h, and 1.5 h after evacuation to 2 × 10^{-8} Torr of O_2 with respect to clean Pt(557) in UHV as the reference, in order to clearly show the XPS peak evolution. The enhancement at +0.2 eV CLS at 10^{-7} Torr shows that only oxygen chemisorption occurs. Surface oxide shoulder at 1 Torr in (a) is now evident in the difference spectrum at +0.6 eV CLS. This oxide component decreases in intensity after O_2 evacuation. (c) Pt 4f spectra of Pt(111) acquired in UHV and under exposure to 1 Torr of O_2 for 2 h. The Pt(111) has a less pronounced surface oxide shoulder than Pt(557), illustrating the relatively high activity of the stepped surface for the formation of the surface oxide phase. (d) Difference Pt 4f spectra of Pt(111) obtained under the same conditions as those in (b) using clean Pt(111) in UHV as the reference. The XPS spectra of Pt(111) evolve similarly to those of Pt(557) but to a less degree owing to the lower step density. All the spectra were recorded with 340 eV photon energy at 298 K and binding energies were calibrated to the Fermi level at 0 eV under the same conditions.

clearly shown in the difference spectrum in Figure 3b. This Pt peak is attributed to surface oxide clusters based on the Pt 4f binding energy, because surface oxides with similar Pt 4f CLS can be formed by exposing stepped or kinked Pt single crystal surfaces to O_2.[26−28] The surface Pt oxide component does not shift in position but only increases in intensity after continued exposure to 1 Torr of O_2 from 40 min to 2 h. This phenomenon indicates that the clusters grow from 1D to 2D without any change in chemical structure. Given that the Pt $4f_{7/2}$ CLS is +1.0−1.3 and +2.2−2.9 eV for PtO and PtO_2, respectively,[38−41] it should be noted that no bulk Pt oxide has formed under our experimental conditions. In addition, the position of the dips in the Pt 4f difference spectra at 70.6 eV (−0.4 eV CLS) is in agreement with Pt atoms in the topmost layer,[26,27,38] which shows the oxide forms at the expense of surface Pt atoms.

In order to investigate the role of steps in creating clusters, the changes of the Pt(111) surface structure in the presence of O_2 were studied as well. Figure 2c, acquired 1.5 h after filling the HP-STM cell with 1 Torr of O_2, shows that a number of clusters have accumulated near the steps edges. The presence of steps on the Pt(111) crystal is due to a miscut angle of approximately 1°, which results in terraces of 12 nm wide on average. Although a few clusters appear on inner terraces, over 90% of the nanometer-sized clusters are located less than 2 nm away from the step edges. This phenomenon is consistent with previous reports that indicate cluster nucleation begins at step sites,[42] owing to the high mobility and activity of low-coordination Pt atoms. Growth of 2D surface Pt oxide is thus more likely to occur on Pt(557) because of the narrow terrace width (1.4 nm) and the high step density. Direct oxidation of Pt(111) terraces by O_2, in contrast, occurs slowly at similar pressures at room temperature, and was reported to happen only above 520 K.[43] By zooming in on the terraces, a hexagonal pattern is resolved between clusters, as marked by the green triangles in Figure 2d. The periodicity of the hexagonal pattern is 590 pm, corresponding to a chemisorbed oxygen p(2 × 2) structure. Since a p(2 × 1) order was observed as the precursor state of Pt oxide on Pt(111) terraces when oxidized by strong oxidants,[44] the p(2 × 2) pattern in our experiments in turn substantiates the slow kinetics of oxidation on terraces.

Pt 4f spectra of Pt(111) also demonstrate the low activity of terraces relative to steps in forming surface oxide. As shown in Figure 3c,d, exposure to 1 Torr of O_2 for 2 h also results in a

dx.doi.org/10.1021/nl204242s | Nano Lett. 2012, 12, 1491−1497

new component on Pt(111) at 71.6 eV (+0.6 eV CLS), the same position as the surface oxide component on Pt(557). The surface oxide formed on Pt(111) is thus indistinguishable from the oxide clusters on Pt(557) based on the same Pt 4f CLS value. However, the increase of intensity at 71.6 eV for Pt(111) on exposure to 1 Torr of O_2 is only one-third of the increase observed on Pt(557), which is in good agreement with the smaller number of clusters seen on Pt(111) by STM. This difference between Pt(111) and Pt(557) is undoubtedly the consequence of the lower step density on Pt(111).

Figure 4a shows that 1.5 h after evacuating O_2 from 1 Torr to 10^{-8} Torr, almost all of the 2D surface oxide clusters disappear

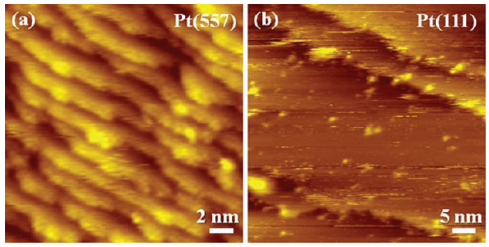

Figure 4. STM images of (a) Pt(557) and (b) Pt(111) 1.5 h after evacuating the HP-STM cell to 10^{-8} Torr. Most clusters have disappeared on both crystals, and steps as well as terraces reappear. V_s = 0.20 V, I_t = 0.10 nA, T = 298 K.

with steps forming again on the Pt(557), although some of the steps are no longer as straight as they originally were on the clean Pt(557) surface in Figure 1. The 1D oxide chains are not observed at the step edges in Figure 4a, however it can be due to the inevitable loss of resolution by the blunting of the STM tip after exposure to 1 Torr of O_2 for several hours. Similarly, very few clusters are left on Pt(111) 1.5 h after evacuating O_2 from 1 Torr to 10^{-8} Torr, as shown in Figure 4b. The removal of surface oxide can be observed by XPS as well. As shown by Pt 4f difference spectra of the Pt(557) in Figure 3b, evacuation of the XPS chamber from 1 Torr to 2×10^{-8} Torr of O_2 causes a significant decrease in intensity of the oxide component at 71.6 eV. Figure 3d reveals that on Pt(111) the peak at 71.6 eV has also nearly disappeared, accompanied with the disappearance of clusters in the STM images.

The disappearance of the 2D oxide clusters upon O_2 evacuation is worth discussing. Given that Pt oxide decomposition and oxygen desorption occur slowly on Pt at room temperature[45] and that a thin Pt oxide film is thermodynamically more stable than bulk Pt oxide,[46] it would be surprising that the 2D oxide decomposed within 1.5 h of O_2 gas removal. However, reactions between surface oxide and background gases (CO and H_2) are likely responsible for removing the 2D oxide, because CO quickly reduces surface Pt oxide even at 273 K.[26,31] Further in situ experiments are planned to study in detail the reaction of 2D oxide with H_2 and CO on Pt(557). Such studies could help investigate whether some distinct structures would appear in these types of reaction mixtures and how the surface structures would differ from oxidizing to reducing conditions by varying the O_2/CO and O_2/H_2 pressure ratios.

To further explore the reactivity toward O_2 of step Pt sites, we also investigated the structure of the Pt(557) surface at low O_2 pressures by means of direct dosing gases from UHV. When exposing clean Pt(557) to 10^{-7} Torr of O_2 at room temperature, periodic bright spots are resolved at parts of the step edges, as revealed in Figure 5. The average spacing of 580 pm is close to twice the Pt−Pt distance in the lattice. Although

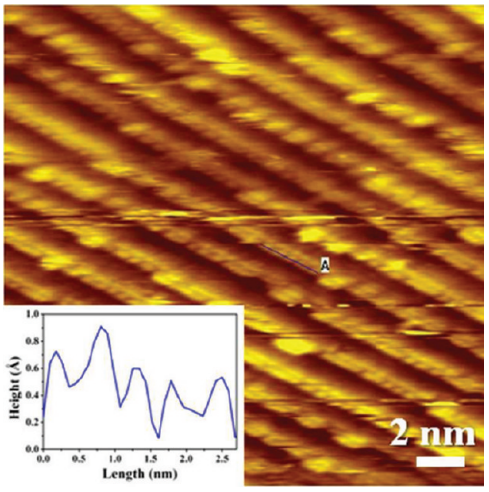

Figure 5. STM images of Pt(557) at 10^{-7} Torr of O_2. Chemisorbed patterns are resolved as bright dots at parts of the step edges. A line profile of the chemisorbed structure is shown in the inset. V_s = 0.20 V, I_t = 0.10 nA, T = 298 K.

we cannot obtain atomic information on the narrow terraces near the step bottom owing to the large tip radius, our results agree with previous STM reports that O_2 only chemisorbs dissociatively at Pt steps at low pressures.[5,47] No clusters are observed at the step edges until the O_2 pressure is raised to 10^{-3} Torr. Moreover, the difference XPS spectrum in Figure 3b shows that 10^{-7} Torr of O_2 does not lead to the growth of the oxide component at 71.6 eV. Instead, the enhancement of the Pt $4f_{7/2}$ peak is located at 71.2 eV (+0.2 eV CLS). This shift is due to the Pt atoms bonded with chemisorbed oxygen on Pt(111) terraces.[26,28] We therefore can conclude that O_2 dominantly chemisorbs on the Pt(557) surface at low pressures. For the Pt(111) system, consensus has already been reached in the literature that O_2 chemisorbs after dissociation below 10^{-6} Torr at room temperature.[44,48−51]

Quantitative curve fits of Pt 4f core level spectra of the Pt(557) were performed, so as to gain further insight into the Pt oxide formation at high pressures of O_2. Pt 4f spectra were recorded with photon energies of 340 and 475 eV, which produce photoelectrons of ∼270 and ∼405 eV kinetic energy, respectively. The ∼270 eV kinetic energy corresponds to an inelastic mean free path of 0.6 nm and ∼405 eV kinetic energy corresponds to 0.8 nm.[35] The thickness of Pt oxide at surface can then be estimated by measuring the oxide intensity at each surface depth. Selected Pt 4f spectra, which were acquired at 1 Torr and after O_2 evacuation to 2×10^{-8} Torr, are displayed along with fitted peaks in Figure 6. These Pt 4f spectra were deconvoluted using asymmetric Voigt-type line-shapes, preceded by a subtraction of the Shirley-type background.[52] Four components, including bulk Pt (gray), surface Pt (−0.4 eV CLS, yellow), Pt bonded with chemisorbed oxygen (+0.2 eV CLS, blue), and surface oxides of Pt (+0.6 eV CLS, red) were used for peak fitting, and no other components were found to be necessary for a good fit. The CLS values of the chemisorbed and surface oxide components are determined from the difference spectra in Figure 3b. Under both O_2 pressures, the intensity ratio of Pt oxide to bulk Pt at 475 eV photon energy is lower than that at 340 eV photon energy. The Pt peak from the

dx.doi.org/10.1021/nl204242s | Nano Lett. 2012, 12, 1491−1497

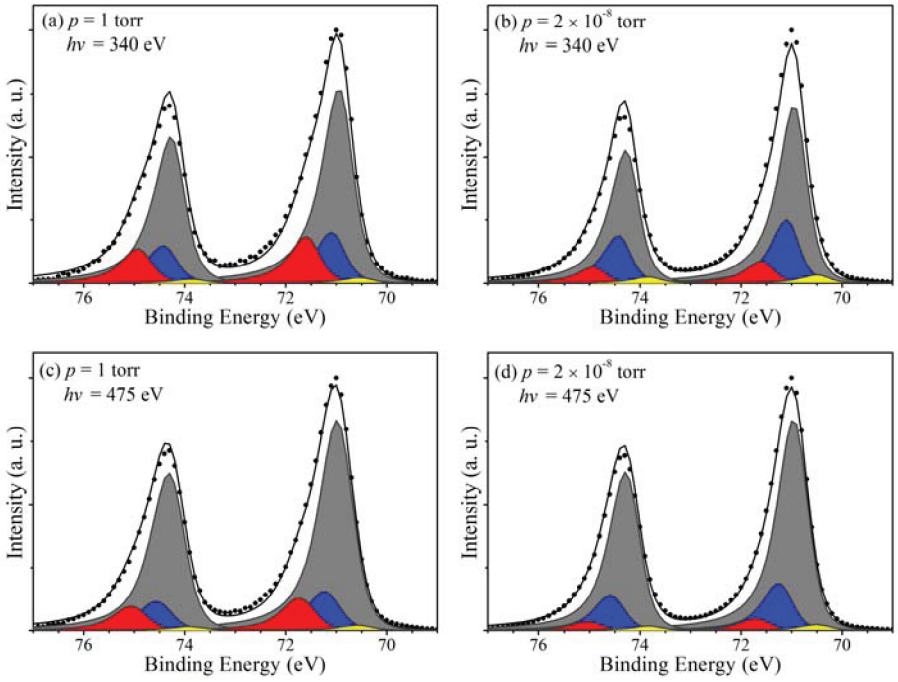

Figure 6. Pt 4f spectra of Pt(557) obtained at 298 K under 2 h exposure to 1 Torr of O_2 and 1.5 h after evacuation to 2×10^{-8} Torr with X-ray energies of 340 eV (probing depth ~0.6 nm) and 475 eV (probing depth ~0.8 nm). Gray, yellow, blue, and red components represent bulk Pt, surface Pt, Pt bonded with chemisorbed oxygen, and Pt in surface oxide, respectively. The black dots denote the raw data points and the gray lines are the fitted spectra (the summation of the gray, yellow, blue, and red components). The fitting results show that surface oxide decomposes upon O_2 evacuation (left to right) and that the oxide is only a surface phase (top to bottom).

chemisorption phase that forms exclusively at the surface decreases in intensity with increasing probing depth as expected. The lower intensity of the oxide peak with deeper probing depth thereby implies that the oxide is only enriched at surface. Although bulk PtO_2 and Pt_3O_4 are both thermodynamically stable at room temperature even at low O_2 pressures,[53,54] growth of surface oxide to form bulk oxide can be kinetically limited by the high energy barrier for oxygen diffusion into the Pt subsurface at room temperature.[55]

The area ratio of Pt in oxide phase to total detected Pt on the Pt(557) sample was then determined by integrating the peak areas of Pt oxide and total Pt in the fitted Pt 4f spectra at both photon energies. The values of surface oxide concentration while switching between high and low pressures of O_2 are plotted in Figure 7. As shown by the red circles and triangles, at 10^{-3} Torr of O_2 when oxide clusters start to appear at Pt step sites in the STM images, the concentrations of Pt oxide at ~0.6 and ~0.8 nm depths are ~6 and ~4%, respectively. The respective Pt oxide ratios at ~0.6 and ~0.8 nm increase to ~15 and ~11% after introducing O_2 to 1 Torr and then decrease to ~7 and ~4% upon evacuating to 2×10^{-8} Torr. Since the Pt oxide concentrations determined by incident energy of 340 eV are always higher than those by 475 eV, the oxide clusters are obviously more populated at the surface. Reintroduction and re-evacuation of O_2 to similar pressures change the Pt oxide concentration at ~0.6 nm to ~15 and ~8%, respectively. Similarly, at ~0.8 nm probing depth, the Pt oxide concentration increases to ~11% upon reintroduction, followed by declining to ~5% after re-evacuation. Such variation in oxide concentration at the surface with changing O_2 pressure can be repeated for several cycles.

Moreover, the oxygen coverage on Pt(557) shows a similar variation in response to changes in O_2 gas pressure. The oxygen

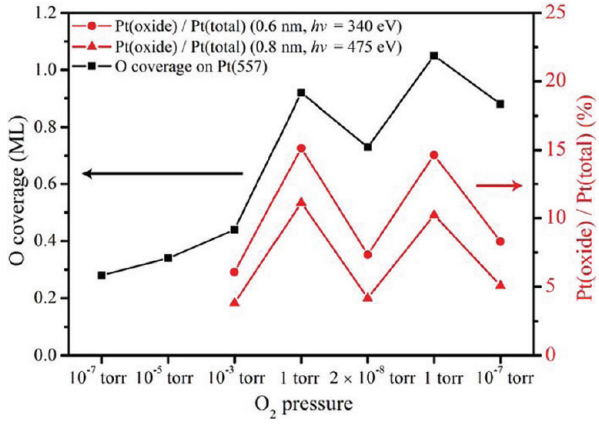

Figure 7. Changes in surface Pt oxide concentration for Pt(557) in response to O_2 pressure variation, as measured with 340 eV (red circles) and 475 eV (red triangles) incident X-ray photon energies. The curves show that changes in surface oxide concentration correlate with changes in the O_2 gas pressure. Black lines: Oxygen coverage on Pt(557) determined from Pt 4f and O 1s photoelectrons (both ~270 eV kinetic energy) after calibration with respect to the 0.25 ML (2×2) structure formed on Pt(111) at 10^{-7} Torr of O_2. Oxygen coverage on Pt(557) varies with gas pressure in a similar trend to that of oxide concentration but gradually increases as a result of surface roughening.

coverage was measured by integration of Pt 4f and O 1s peak areas (both recorded with ~270 eV kinetic energy photoelectrons), and a subsequent calibration using the oxygen coverage of 0.25 ML on Pt(111) at 10^{-7} Torr.[48−51] At 10^{-7} Torr, the oxygen coverage on Pt(557) is 0.28 ML and then slowly increases with O_2 pressure until 0.42 ML at 10^{-3} Torr. The coverage suddenly increases to 0.93 ML at 1 Torr. A similar experiment on Pt(111) gives the coverage of 0.48 ML at

dx.doi.org/10.1021/nl204242s | Nano Lett. 2012, 12, 1491−1497

1 Torr of O_2. The large difference in oxygen coverage between Pt(557) and Pt(111) is indicative of the higher activity of step sites as compared to terrace atoms in forming Pt oxide. After O_2 gas evacuation, the oxygen coverage on Pt(557) remains stable at 0.70 ML. However, this value is still larger than the 0.28 ML seen after initial exposure to 10^{-7} Torr. The oxygen coverage on Pt(557) then increases to 1.05 ML upon reintroduction of O_2 to 1 Torr and decreases to 0.82 ML after re-evacuation. Changes in oxygen coverage can also be repeated over several cycles and are in agreement with the variation in surface oxide concentration.

In conclusion, we performed in situ STM and XPS studies to monitor the structural and chemical evolution of a stepped Pt(557) surface in the presence of high pressures (1 Torr) of O_2 at room temperature. STM images illustrate that at 1 Torr, periodic 1D chains form initially at step edges, which is followed by the formation of a large number of nanometer-sized clusters as O_2 exposure time increases. The clusters are identified as surface Pt oxide by their high-binding energy component at +0.6 eV with respect to the metallic Pt peak in XPS spectra obtained under the same conditions. In a comparative experiment on Pt(111), both HP-STM and AP-XPS demonstrate that low-coordinated step atoms are more active than terrace sites in reacting with O_2. Most clusters disappear on both Pt(557) and Pt(111) upon evacuation of O_2 to 10^{-8} Torr. Such dramatic structural changes on the stepped Pt(557) surface are seen only when the O_2 gas pressure reaches 1 Torr, whereas at low pressures, such as 10^{-7} Torr, only chemisorption occurs. Our results indicate that it is important to study the structure of stepped Pt single crystal model catalysts under ambient pressures, not only since they can undergo dramatic structure changes in equilibrium with high-pressures of gas phase reactants, but also because the high structural flexibility of stepped Pt surfaces allows us to bridge the connection between surface structures and catalytic performances.

■ ASSOCIATED CONTENT

Supporting Information

Additional information and figures. This material is available free of charge via the Internet at http://pubs.acs.org.

■ AUTHOR INFORMATION

Corresponding Author

*E-mail: somorjai@berkeley.edu.

Notes

The authors declare no competing financial interest.

■ ACKNOWLEDGMENTS

We acknowledge Dr. Simon Beaumont, Dr. Vladimir Pushkarev, Yu Shi, and Xiaofeng Feng for helpful discussions. This work was supported by the Director, Office of Science, Office of Basic Energy Sciences, Materials Sciences and Engineering Division, of the U.S. Department of Energy under Contract No. DE-AC02-05CH11231.

■ REFERENCES

(1) Somorjai, G. A.; Li, Y. *Introduction to Surface Chemistry and Catalysis*, 2nd ed.; Johns Wiley & Sons, Inc.: Hoboken, NJ, 2010.
(2) Ertl, G.; Knözinger, H.; Schüth, F.; Weitkamp, J. *Handbook of Heterogeneous Catalysis*, 2nd ed.; Wiley-VCH: Weinheim, 2008.
(3) Hendriksen, B. L. M.; Ackermann, M. D.; van Rijn, R.; Stoltz, D.; Popa, I.; Balmes, O.; Resta, A.; Wermeille, D.; Felici, R.; Ferrer, S.; Frenken, J. W. M. *Nature Chem.* **2010**, *2*, 730−734.
(4) Zambelli, T.; Wintterlin, J.; Trost, J.; Ertl, G. *Science* **1996**, *273*, 1688−1690.
(5) Gambardella, P.; Šljivančanin, Ž.; Hammer, B.; Blanc, M.; Kuhnke, K.; Kern, K. *Phys. Rev. Lett.* **2001**, *87*, 056103.
(6) Hammer, B.; Nielsen, O. H.; Nørskov, J. K. *Catal. Lett.* **1997**, *46*, 31−35.
(7) Vang, R. T.; Honkala, K.; Dahl, S.; Vestergaard, E. K.; Schnadt, J.; Lægsgaard, E.; Clausen, B. S.; Nørskov, J. K.; Besenbacher, F. *Nat. Mater.* **2005**, *4*, 160−162.
(8) Batteas, J. D.; Dunphy, J. C.; Somorjai, G. A.; Salmeron, M. *Phys. Rev. Lett.* **1996**, *77*, 534−537.
(9) Lindauer, G.; Légaré, P.; Maire, G. *Surf. Sci.* **1983**, *126*, 301−306.
(10) Hahn, E.; Schief, H.; Marsico, V.; Fricke, A.; Kern, K. *Phys. Rev. Lett.* **1994**, *72*, 3378−3381.
(11) Sander, M.; Imbihl, R.; Schuster, R.; Barth, J. V.; Ertl, G. *Surf. Sci.* **1992**, *271*, 159−169.
(12) Tao, F.; Dag, S.; Wang, L. W.; Liu, Z.; Butcher, D. R.; Bluhm, H.; Salmeron, M.; Somorjai, G. A. *Science* **2010**, *327*, 850−853.
(13) Montano, M.; Bratlie, K. M.; Salmeron, M.; Somorjai, G. A. *J. Am. Chem. Soc.* **2006**, *128*, 13229−13234.
(14) Li, Y.; Liu, J. H.-C.; Witham, C. A.; Huang, W.; Marcus, M. A.; Fakra, S. C.; Alayoglu, P.; Zhu, Z.; Thompson, C. M.; Arjun, A.; Lee, K.; Gross, E.; Toste, F. D.; Somorjai, G. A. *J. Am. Chem. Soc.* **2011**, *133*, 13527−13533.
(15) Grass, M. E.; Zhang, Y.; Butcher, D. R.; Park, J. Y.; Li, Y.; Bluhm, H.; Bratlie, K. M.; Zhang, T.; Somorjai, G. A. *Angew. Chem., Int. Ed.* **2008**, *47*, 8893−8896.
(16) Zheng, F.; Alayoglu, S.; Guo, J.; Pushkarev, V.; Li, Y.; Glans, P. A.; Chen, J. L.; Somorjai, G. A. *Nano Lett.* **2011**, *11*, 847−853.
(17) Ackermann, M. D.; Pedersen, T. M.; Hendriksen, B. L. M.; Robach, O.; Bobaru, S. C.; Popa, I.; Quiros, C.; Kim, H.; Hammer, B.; Ferrer, S.; Frenken, J. W. M. *Phys. Rev. Lett.* **2005**, *95*, 255505.
(18) Hendriksen, B. L. M.; Frenken, J. W. M. *Phys. Rev. Lett.* **2002**, *89*, 046101.
(19) Tao, F.; Dag, S.; Wang, L. W.; Liu, Z.; Butcher, D. R.; Salmeron, M.; Somorjai, G. A. *Nano Lett.* **2009**, *9*, 2167−2171.
(20) Thostrup, P.; Vestergaard, E. K.; An, T.; Lægsgaard, E.; Besenbacher, F. *J. Chem. Phys.* **2003**, *118*, 3724−3730.
(21) Österlund, L.; Rasmussen, P. B.; Thostrup, P.; Lægsgaard, E.; Stensgaard, I.; Besenbacher, F. *Phys. Rev. Lett.* **2001**, *86*, 460−463.
(22) Somorjai, G. A.; Park, J. Y. *Angew. Chem., Int. Ed.* **2008**, *47*, 9212−9228.
(23) Vang, R. T.; Lægsgaard, E.; Besenbacher, F. *Phys. Chem. Chem. Phys.* **2007**, *9*, 3460−3469.
(24) Salmeron, M.; Schlögl, R. *Surf. Sci. Rep.* **2008**, *63*, 169−199.
(25) Longwitz, S. R.; Schnadt, J.; Vestergaard, E. K.; Vang, R. T.; Lægsgaard, E.; Stensgaard, I.; Brune, H.; Besenbacher, F. *J. Phys. Chem. B* **2004**, *108*, 14497−14502.
(26) Wang, J. G.; Li, W. X.; Borg, M.; Gustafson, J.; Mikkelsen, A.; Pedersen, T. M.; Lundgren, E.; Weissenrieder, J.; Klikovits, J.; Schmid, M.; Hammer, B.; Andersen, J. N. *Phys. Rev. Lett.* **2005**, *95*, 256102.
(27) Held, G.; Jones, L. B.; Seddon, E. A.; King, D. A. *J. Phys. Chem. B* **2005**, *109*, 6159−6163.
(28) Günther, S.; Scheibe, A.; Bluhm, H.; Haevecker, M.; Kleimenov, E.; Knop-Gericke, A.; Schlögl, R.; Imbihl, R. *J. Phys. Chem. C* **2008**, *112*, 15382−15393.
(29) Bandlow, J.; Kaghazchi, P.; Jacob, T.; Papp, C.; Tränkenschuh, B.; Streber, R.; Lorenz, M. P. A; Fuhrmann, T.; Denecke, R.; Steinrück, H. P. *Phys. Rev. B* **2011**, *83*, 174107.
(30) Li, W. X.; Österlund, L.; Vestergaard, E. K.; Vang, R. T.; Matthiesen, J.; Pedersen, T. M.; Lægsgaard, E.; Hammer, B.; Besenbacher, F. *Phys. Rev. Lett.* **2004**, *93*, 146104.
(31) Butcher, D. R.; Grass, M. E.; Zeng, Z.; Aksoy, F.; Bluhm, H.; Li, W.-X.; Mun, B. S.; Somorjai, G. A.; Liu, Z. *J. Am. Chem. Soc.* **2011**, *133* (50), 20319−20325.

(32) Tao, F.; Tang, D. C.; Salmeron, M.; Somorjai, G. A. *Rev. Sci. Instrum.* **2008**, *79*, 084101.
(33) Grass, M. E.; Karlsson, P. G.; Aksoy, F.; Lundqvist, M.; Wannberg, B.; Mun, B. S.; Hussain, Z.; Liu, Z. *Rev. Sci. Instrum.* **2010**, *81*, 053106.
(34) Aksoy, F.; Grass, M. E.; Joo, S. H.; Jabeen, N.; Hong, Y. P.; Hussain, Z.; Mun, B. S.; Liu, Z. *Nucl. Instrum. Methods Phys. Res., Sect. A* **2011**, *645*, 260−265.
(35) Powell, C. J.; Jablonski, A. *NIST Electron Inelastic Mean Free Path Database*, version 1.2; National Institute of Standards and Technology: Gaithersburg, MD, 2010.
(36) Van Hove, M. A.; Somorjai, G. A. *Surf. Sci.* **1980**, *92*, 489−518.
(37) Moulder, J. F.; Stickle, W. F.; Sobol, P. E.; Bomben, K. D. *Handbook of X-ray Photoelectron Spectronscopy*; Perkin-Elmer Corporation: Eden Prarie, MN, 1992.
(38) Légaré, P.; Lindauer, G.; Hilaire, L.; Maire, G.; Ehrhardt, J. J.; Jupille, J.; Cassuto, A.; Guillot, C.; Lecante, J. *Surf. Sci.* **1988**, *198*, 69−78.
(39) Hecq, M.; Hecq, A.; Delrue, J. P.; Robert, T. *J. Less Common Metals* **1979**, *64*, P25−P37.
(40) Hilaire, L.; Guerrero, G. D.; Légaré, P.; Maire, G.; Krill, G. *Surf. Sci.* **1984**, *146*, 569−582.
(41) Peuckert, M.; Bonzel, H. P. *Surf. Sci.* **1984**, *145*, 239−259.
(42) Krasnikov, S. A.; Murphy, S.; Berdunov, N.; McCoy, A. P.; Radican, K.; Shvets, I. V. *Nanotechnology* **2010**, *21*, 335301.
(43) Miller, D. J.; Öberg, H.; Kaya, S.; Sanchez Casalongue, H.; Friebel, D.; Anniyev, T.; Ogasawara, H.; Bluhm, H.; Pettersson, L. G. M.; Nilsson, A. *Phys. Rev. Lett.* **2011**, *107*, 195502.
(44) Devarajan, S. P.; Hinojosa, J. A. Jr; Weaver, J. F. *Surf. Sci.* **2008**, *602*, 3116−3124.
(45) Weaver, J. F.; Chen, J.-J.; Gerrard, A. L. *Surf. Sci.* **2005**, *592*, 83−103.
(46) Campbell, C. T. *Phys. Rev. Lett.* **2006**, *96*, 066106.
(47) Feibelman, P. J.; Esch, S.; Michely, T. *Phys. Rev. Lett.* **1996**, *77*, 2257.
(48) Gland, J. L.; Sexton, B. A.; Fisher, G. B. *Surf. Sci.* **1980**, *95*, 587−602.
(49) Materer, N.; Starke, U.; Barbieri, A.; Döll, R.; Heinz, K.; Van Hove, M. A.; Somorjai, G. A. *Surf. Sci.* **1995**, *325*, 207−222.
(50) Parker, D. H.; Bartram, M. E.; Koel, B. E. *Surf. Sci.* **1989**, *217*, 489−510.
(51) Puglia, C.; Nilsson, A.; Hernnäs, B.; Karis, O.; Bennich, P.; Mårtensson, N. *Surf. Sci.* **1995**, *342*, 119−133.
(52) Shirley, D. A. *Phys. Rev. B* **1972**, *5*, 4709−4714.
(53) Salmeron, M.; Brewer, L.; Somorjai, G. A. *Surf. Sci.* **1981**, *112*, 207−228.
(54) Seriani, N.; Pompe, W.; Ciacchi, L. C. *J. Phys. Chem. B* **2006**, *110*, 14860−14869.
(55) Gu, Z.; Balbuena, P. B. *J. Phys. Chem. C* **2007**, *111*, 9877−9883.